**Fig. 3** Enhanced osteoblastic phenotypes on the sputtered HA surface. A quantitative analysis of ALP activity was performed by normalizing total ALP amount by total DNA content (a). The Alizarin *red* positive staining is represented as percentages of the total culture area (b). mRNA expression levels of osteoblast-related genes (c–g), where x-axis represent days of culture, and y-axis represent expression levels relative to Ti group of the first time point. Data are shown as the mean ± SD ($n = 6$). Statistically different between HA and Ti groups (*$P < 0.05$, **$P < 0.01$)
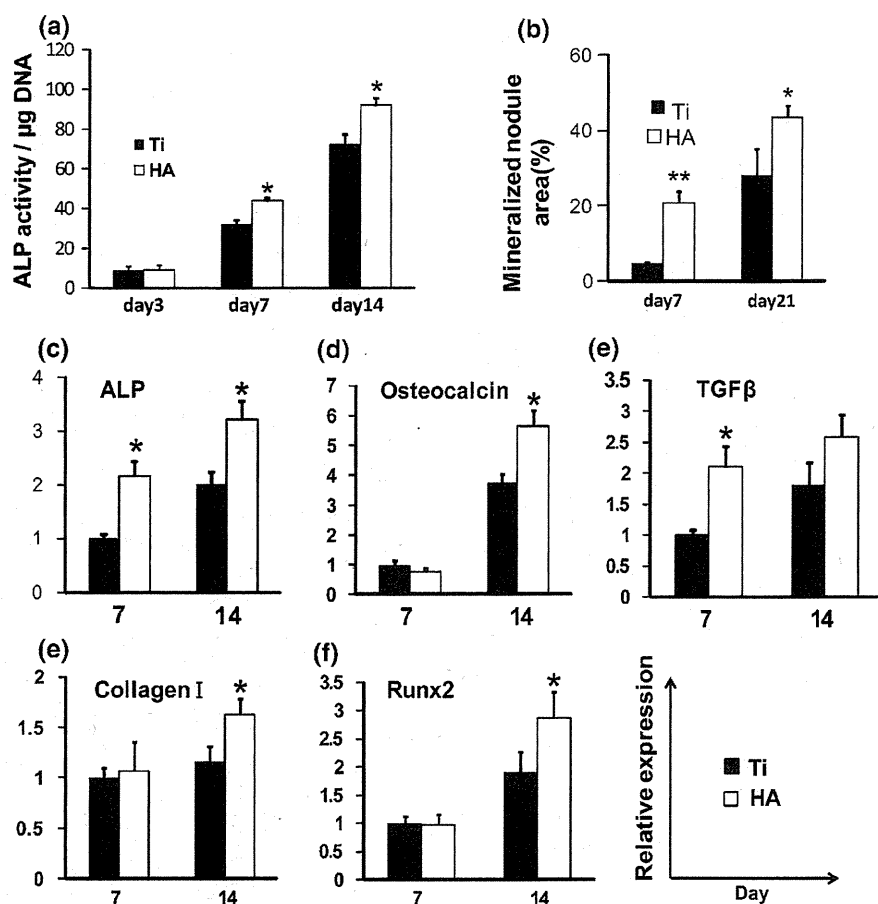

the cell number might be reflected by emphasized BrdU incorporation on the HA at day 2 (68% higher than on the Ti surface). These current results indicated that the sputtered HA surface could significantly enhance the bone marrow stromal cells compared with Ti surface. Since the surface of the sputtered HA and the titanium was manufactured with similar roughness, the enhanced proliferation on the HA may have been due to the difference in the chemical composition of the coating.

ALP expression is associated with osteoblastic differentiation and the level of ALP activity indicates the stage of osteoblastic differentiation. In the present study, the ALP activity was significantly elevated on the sputtered HA surface than on the Ti surface from day 7. This is in line with the previous study that hydrothermally treated sputtered HA film could promote the ALP activity of MC3T3-E1 osteoblast-like cells after 96 h culture [11]. The significantly increased gene expression levels of collagen I, runx2, osteocalcin and ALP on the sputtered HA surface further supported the results. Furthermore, the mineralized nodule deposition on HA was 1.8 times as extensive as that on Ti ($P < 0.05$), indicating that the sputtered HA surface provided a favorable surface for

bone marrow cell adhesion, proliferation and osteoblast differentiation.

Osteoclast is the principal cell responsible for the resorption of bone during bone remodeling. The organization of the actin cytoskeleton plays an important role in the resorption function of osteoclasts. Depending on the substratum upon which the osteoclasts spread, actin presents flat podosomes or sealing zone. It has been reported that when osteoclasts adhere on plastic or glass, podosomes are arranged at the osteoclast periphery as a characteristic belt. If adhering to a mineralized matrix, osteoclasts polarize and exhibit a typical sealing zone which delineates the ruffled border, a site of active membrane traffic and transport, where protons and proteases are secreted in order to dissolve minerals by acidification and degrade extracellular matrix proteins. A large surface area ($>3{,}000 \ \mu m^2$) corresponded to spreading of non-resorbing osteoclasts without sealing zone. In contrast, cell surfaces between 1,700 and 2,000 μm^2 corresponded to actively resorbing osteoclasts exhibiting a sealing zone [18]. In the present study, the osteoclasts on the HA surface always showed smaller size compared with those on the Ti and the polystyrene culture wells, but close to that on the dentine. The

Fig. 4 Osteoclast formation and cytoskeletal arrangement. Micrographs show osteoclastic differentiation on HA (**a**, **b**), dentine (**c**, **d**), Ti (**e**, **f**) and control polystyrene culture wells (**g**, **h**) at co-culture day 5. Cells were stained with DAPI for nuclei (*blue*) and phalloidin for actin filaments (*green*) (**a**, **c**, **e**, **g**) and with TRAP (**b**, **d**, **f**, **h**). Sealing zones, represented by actin rings were indicated by *arrows*, and prodosome belts were indicated by *arrow heads*
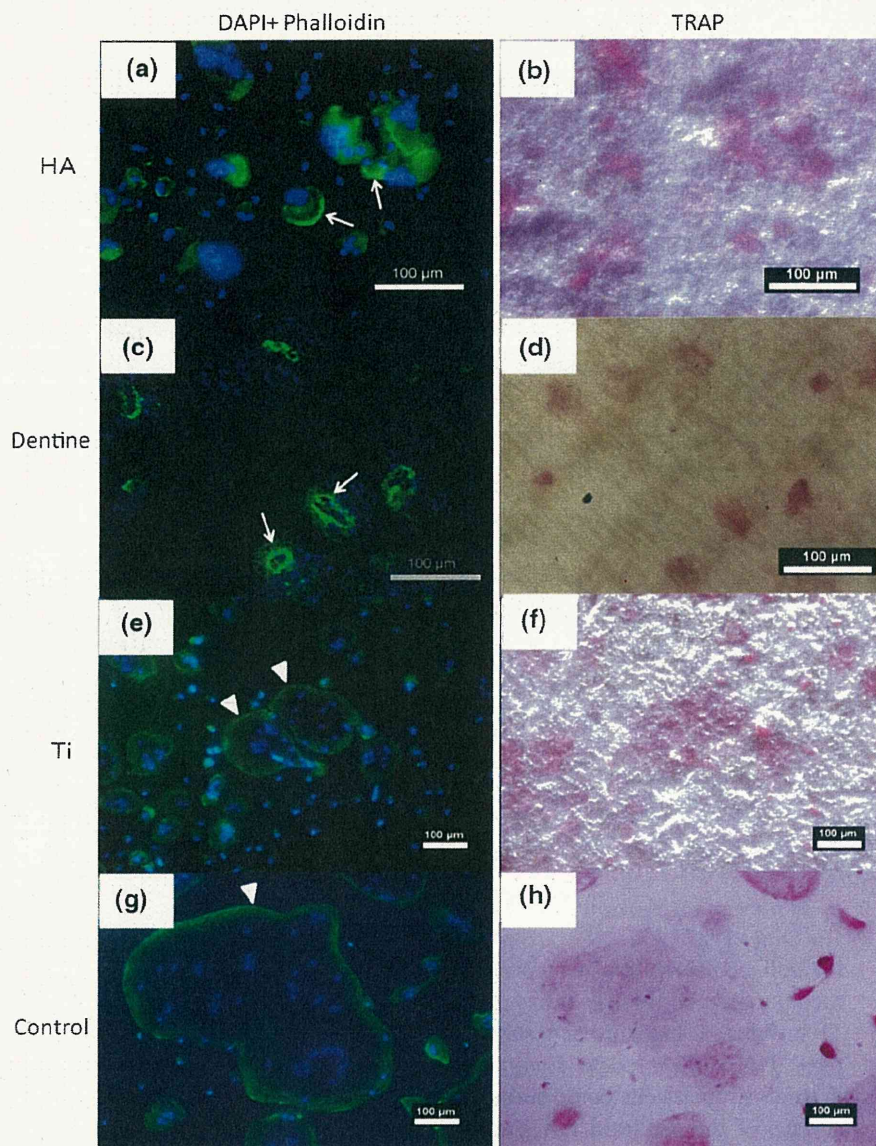
typical podosome belt structure represented as actin dots was found at the periphery of the osteoclast on the Ti and the polystyrene culture wells. However, on both the HA coating and dentine surfaces, a much denser but smaller actin ring structure-sealing zone was shown. These results were also consistent with the previous finding that the size of each actin dot within the sealing zone on a mineralized matrix is four times larger than that on plastic or glass surface [18]. From these results it could be suggested that osteoclast formed on the sputtered HA surface could apico-basal polarize, and exhibit a typical sealing zone, inside of which the active resorption takes place. The osteoclasts formed on the sputtered HA surface could have a similar morphology and behavior to those on the dentine. And the element distribution of the HA coating was further ana-lyzed by EDS mapping, confirming that $32.3 \pm 3.5\%$ of

the sputtered HA coating area degradation was mediated by osteoclastic resorption.

During the differentiation of the progenitor cells to osteoclasts, a series of osteoclast markers were analyzed. TRAP is highly expressed in osteoclasts, and the secretion of TRAP by osteoclasts represents the rate of resorptive activity [19]. CTR is regarded as the best late-stage dif-ferentiation marker for osteoclasts, which distinguishes them from macrophage polykaryons [20]. During osteo-clastic resorption, hard tissues are demineralized by v-ATPase [21] and collagens are subsequently degraded by cathepsin K [22] and MMP-9 [23]. In the present study, TRAP and CTR were expressed at significantly higher levels on HA than on Ti at day 7. v-ATPase expression level was increased on HA at day 5. However, no differ-ences could be observed in terms of Cathepsin K and

chewing complaint without replacement of edentulous space, and this may have contributed to the significantly greater percentage of subjects in this group with untreated SDA longer than 1 year.

Asymmetric arch was a significant factor for the perception of chewing complaint as well as for prosthetic restoration $(P < 0.01)$. This suggests that impairment of chewing ability owing to asymmetry of the arch could lead to prosthetic restoration. Käyser reported (1) that subjects started complaining about chewing function when the number of remaining OU became <4 in a symmetrical arch or <6 in asymmetric arch. This indicates that the shorter side of an asymmetric SDA has more negative impact on perceived chewing ability than symmetrical SDA. The results of our study confirm this finding. In our study, subjects with symmetrical SDA did not have a preferred chewing side, while 63% of subjects with asymmetric SDA preferred to chew on the longer side. Unilateral chewing owing to asymmetry of the arch may be responsible for chewing complaint.

The mean age of the IFPD group was significantly lower than those for no-treatment group and RPD group $(P < 0.05)$, and percentage of male subjects in IFPD group was significantly greater than in RPD group and no-treatment group $(P = 0.044)$. These suggest that age and gender were associated with the choice of RPD or IFPD. The Japanese national health insurance system covers most of the cost for treatment with acrylic resin-based RPD, but not for IFPD. Patients in Japan can receive acrylic resin-based RPD treatment at a much reduced fee compared to the IFPD. Thus, the large difference in treatment cost between PRD and IFPD possibly confounded the age and gender effect. Younger male SDA patients may have higher income, and they spend their own money to IFPD treatment, while elderly female SDA patients prefer RPD treatment because of lower income. Several epidemiological studies have shown that socio-economic status defined as an economic and sociological combined total measure of a person's work experience and of an individual's or family's economic and social position relative to others, based on income, education and occupation, was closely associated with frequencies and type of prosthetic restorations in European countries (27). The aforementioned factors may have influenced the decision-making for prosthetic treatment with RPD or IFPD in the present study. It is necessary to carry out further studies with multivariate analysis to clarify whether treatment cost and socio-economic status of patients are associated with the choice of prosthetic treatment with RPD or IFPD.

In this study, the allocation of options, no treatment or treatment with RPD or IFPD, was not randomised but primarily patients' preference. Therefore, homogeneity of characteristics among groups could not be assumed. In fact, significant differences between groups were found in mean age and number of missing OU, distribution in gender, and duration of SDA without replacement. These factors possibly act as confounding factors in comparisons of the measures between groups, and thus, they should be controlled statistically when comparing outcome measures between groups. The subjects were recruited from university-based dental hospitals. About 40% of subjects did not seek prosthetic treatment in their edentulous space. It is not known whether this percentage is applicable to those in SDA patients who visit private dental offices.

Acknowledgments

References

1. Käyser AF. Shortened dental arches and oral function. J Oral Rehabil. 1981;8:457–462.
2. Kanno T, Carlsson GE. A review of the shortened dental arch concept focusing on the work by the Käyser/Nijmegen group. J Oral Rehabil. 2006;33:850–862.
3. Budtz-Jørgensen E, Isidor F. A 5-year longitudinal study of cantilevered fixed partial dentures compared with removable partial dentures in a geriatric population. J Prosthet Dent. 1990;64:42–47.
4. Isidor F, Budtz-Jørgensen E. Periodontal conditions following treatment with distally extending cantilever bridges or removable partial dentures in elderly patients. A 5-year study. J Periondontol. 1990;61:21–26.
5. Jepson NJ, Moynihan PJ, Kelly PJ, Watson GW, Thomason JM. Caries incidence following restoration of shortened lower dental arches in a randomized controlled trial. Br Dent J. 2001;191:140–144.

Predictors	B	s.e.	Wald	P	Odds ratio	95% CI
Gender[*]	−0·724	0·515	1·98	0·160	0·485	0·177–1·329
Age	−0·045	0·021	4·39	0·036	0·956	0·917–0·997
Number of missing OU	0·794	0·159	25·07	<0·001	2·212	1·621–3·019
Chewing complaint[†]	1·224	0·465	6·92	0·009	3·399	1·366–8·459
Symmetry[‡]	2·732	0·758	12·98	<0·001	15·362	3·476–67·898
Constant	−3·148	1·613	3·81	0·051	0·043	

Table 6. Factors related to prosthetic restoration in total subjects (n = 145). No treatment was coded as 0 and prosthetic treatment was coded as 1 for an outcome variable

B, partial regression coefficient; s.e., standard error; CI, confidence interval.
[*]Gender: 0, male; 1, female.
[†]Chewing complaint: 0, absence; 1, presence.
[‡]Symmetry: 0, missing OU on right side is equal to left side (symmetrical SDA); 1, missing OU on right side is not equal to left side (asymmetric SDA).

Predictors	B	s.e.	Wald	P	Odds ratio	95% CI
Gender[*]	−0·344	0·694	0·245	0·620	0·709	0·182–2·762
Age	−0·035	0·026	1·765	0·184	0·966	0·917–1·017
Number of missing OU	0·141	0·329	0·183	0·668	1·151	0·604–2·193
Chewing complaint[†]	1·332	0·581	5·261	0·022	3·791	1·214–11·836
Symmetry[‡]	0·614	1·188	0·267	0·605	1·848	0·180–18·960
Constant	0·946	2·603	0·132	0·716	2·576	

Table 7. Factors related to prosthetic restoration in SDA type II subjects (n = 62). No treatment was coded as 0 and prosthetic treatment was coded as 1 for an outcome variable

B, partial regression coefficient; s.e., standard error; CI, confidence interval.
[*]Gender: 0, male; 1, female.
[†]Chewing complaint: 0, absence; 1, presence.
[‡]Symmetry: 0, missing OU on right side is equal to left side (symmetrical SDA); 1, missing OU on right side is not equal to left side (asymmetric SDA).

Predictors	B	s.e.	Wald	P	Odds ratio	95% CI
Gender[*]	0·478	0·416	1·320	0·251	1·613	0·714–3·646
Age	0·007	0·017	0·166	0·684	1·007	0·973–1·042
Number of missing OU	0·258	0·084	9·414	0·002	1·295	1·098–1·527
Symmetry[†]	1·477	0·517	8·177	0·004	4·380	1·591–12·055
Constant	−3·403	1·327	6·573	0·010	0·033	

Table 8. Factors related to chewing complaint in total subjects (n = 145). As an outcome, absence of chewing complaint was coded as 0 and presence of chewing complaint was coded as 1

B, partial regression coefficient; s.e., standard error; CI, confidence interval.
[*]Gender: 0, male; 1, female.
[†]Symmetry: 0, missing OU on right side is equal to left side (symmetrical SDA); 1, missing OU on right side is not equal to left side (asymmetric SDA).

loss of an occluding pair of first molars is a key factor for choosing prosthetic restoration in SDA patients.

The regression analyses for SDA type II subjects alone, as well as in total subjects, found that the perception of chewing complaint was a significant factor for choosing prosthetic treatment (P < 0·05). In addition, increase in missing OU was a significant factor for the presence of chewing complaint (P = 0·002). Posterior teeth play an important role in comminuting food bolus and mixing with saliva (26). Therefore, impairment of chewing ability owing to missing occluding pairs of posterior teeth is considered to lead to prosthetic restoration. A significantly lower percentage of subjects in no-treatment group complained about chewing ability compared to RPD or IFPD group (P < 0·001). Most of the subjects in the no-treatment group (73%) had no

Table 4. Characteristics of the subjects at baseline (*n* = 145)

		Treatment	
	No treatment	Removable partial denture	Implant-supported fixed partial denture
Number of subjects	59	61	25
Gender (male)	27·1%	18·0%	44·0%
Mean age (s.d.) (years)	64·0 (11·7)	65·0 (9·1)	58·2 (10·2)
Mean number of missing occlusal units (s.d.)	4·1 (2·1)	7·0 (2·4)	5·1 (1·7)
Duration of shortened dental arches (SDA) more than 12 months	72·7%	39·0%	36·0%
Chewing complaint (presence)	27·1%	73·3%	48·0%
Educational level (university or college)	38·2%	33·9%	40·9%
Past usage of RPD (presence)	43·5%	42·6%	40·0%
Symmetry (symmetrical SDA)	27·1%	18·0%	8·0%

complaint as significant predictors for prosthetic restoration (*P* < 0·05) (Table 6). When the analysis was limited to SDA type II subjects, the presence of chewing complaint was identified as the significant predictor for prosthetic restoration (*P* = 0·022) (Table 7). On the other hand, increased numbers of missing OU and asymmetric arch were identified as significant predictors for the presence of chewing complaint (Table 8).

Discussion

A number of intervention studies have been carried out to investigate the effect of treatment with RPD or cantilever-fixed partial dentures in SDA patients (3–8, 12). A randomised clinical trial has been carried out to investigate the effect of prosthetic treatment with RPD or IFPD in partially dentate patients with Kennedy class I or II condition (24). However, to our knowledge, the

Table 5. Distribution of subjects for no-treatment or treatment groups by subtype of shortened dental arches (SDA)

	SDA subtype					
	Type I (*n* = 30)		Type II (*n* = 62)		Type III (*n* = 53)	
	n	%	*n*	%	*n*	%
No treatment	29	96·7	26	41·9	4	7·5
Treatment						
Removable partial denture	0	0·0	21	33·9	40	75·5
Implant-supported fixed partial denture	1	3·3	15	24·2	9	17·0

present study is the first one in SDA patients. When Käyser proposed the SDA concept in the early 1980s (1), IFPD had not been established as a treatment option for SDA patients. Dental implants are becoming increasingly utilised for the replacement of missing teeth in a partially dentate arch. Thus, IFPD was included as a treatment option in the present study when considering prosthetic restoration in SDA patients. On the other hand, treatment with cantilever-fixed partial dentures is limited in Japan when compared to European countries because not all cases are covered by the Japanese national health insurance; for example, second premolar and first molar are abutments, and second molar is a pontic. It was expected to be difficult to obtain an adequate sample size for this option. Thus, cantilever-fixed partial dentures were not included in this study.

As shown in Fig. 1, subjects with more than two missing OUs tended to choose prosthetic treatment. The regression analysis identified an increased number of missing OU as a significant predictor for prosthetic restoration when controlling for age, gender, arch symmetry and perception of chewing complaint (*P* < 0·001). These results support our hypothesis that an increase in missing OU is associated with prosthetic restoration. It has been reported that the occluding pair of first molars provide sufficient OHRQoL (22) and chewing ability measured using a food intake questionnaire (25). In the present study, a great majority of subjects with SDA type I (97%) who missed just second premolar(s) chose no treatment; in contrast, about 60% of SDA type II subjects who missed first and second molars sought prosthetic treatment. This suggests that

restoration. A *P* value <0·05 was considered significant. SPSS 17.0* was used for statistical analyses.

Results

During the period from February 2009 to November 2009, a total of 173 patients met the prescribed criteria, and baseline evaluation was performed in 145 subjects (25–87 years, mean age; 63·4 years, standard deviation; 10·6 years, men; 26·2%). Of these subjects, 40·7% (59/145) chose no treatment, and 59·3% (86/145) sought treatment with an RPD (42·1%: 61/145) or IFPD (17·2%; 25/145). The distribution of subjects for three options in each school is shown in Table 3. Seventy-two per cent (104/145) of the subjects who completed baseline assessment were recruited from three schools in urban areas (Tokyo Medical and Dental University, Osaka University, and Showa University.) and 28% (41/145) from four schools (Kyushu University, Hiroshima University, Okayama University and Tohoku University) in rural areas. Distribution of subjects who choose no treatment was different between seven schools (29–50%). The distribution of subjects by number of missing OU is shown in Fig. 1. Only 4·3% (1/23) of subjects with two missing OUs sought prosthetic treatment. The percentage of subjects who sought prosthetic treatment increased to 53·3% (26/47) in subjects with four missing OUs and 75·8% (50/66) in subjects with 5–9 missing OUs. All subjects with more than nine missing OUs (n = 10) sought prosthetic treatment with RPD.

The characteristics of each group at baseline are presented in Table 4. The IFPD group showed a significantly higher percentage of male subjects (P = 0·044). ANOVA found significant effects of group on age (F = 3·9, P = 0·022) and number of missing OU (F = 27·0, P < 0·001). Tukey's test found that the mean age in IFPD group was less than those in no-treatment group and RPD group (P < 0·05) and that the mean number of missing OUs in the RPD group was significantly greater than that in the no-treatment group and IFPD group (P < 0·01). The no-treatment group showed a greater percentage of subjects whose edentulous space had not been replaced for more than 12 months, compared to the RPD and IFPD groups (P < 0·01). The RPD group showed a significantly higher percentage of subjects who complained about chewing ability compared to the

*SPSS Japan Inc., Tokyo, Japan.

Table 3. Distribution of subjects in seven dental schools at baseline assessment (n = 145). Numbers in parentheses indicate percentage of subjects who choose no treatment or treatment with removable partial denture (RPD) or implant-supported fixed partial dentures (IFPD) in each school

Dental school	n	No treatment (%)	Treatment RPD (%)	IFPD (%)
Tokyo Medical and Dental University	60	29 (48·3)	29 (48·3)	2 (3·3)
Osaka University	24	8 (33·3)	5 (20·8)	11 (45·8)
Showa University	20	8 (40·0)	9 (45·0)	3 (15·0)
Kyushu University	17	5 (29·4)	9 (52·9)	3 (17·6)
Hiroshima University	10	5 (50·0)	4 (40·0)	1 (10·0)
Tohoku University	7	2 (28·6)	3 (42·9)	2 (28·6)
Okayama University	7	2 (28·6)	2 (28·6)	3 (42·9)
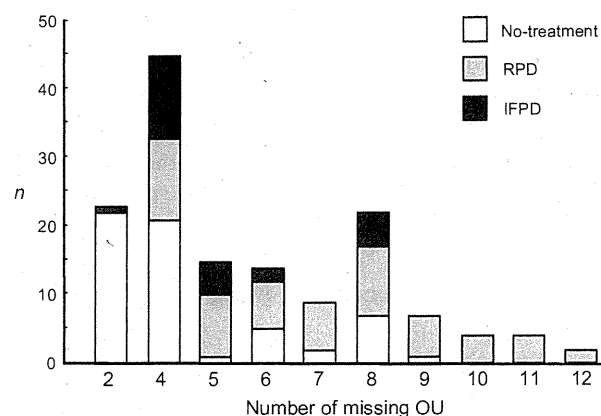
Fig. 1. Distribution of subjects with shortened dental arches by number of missing OU and prosthetic restoration.

no-treatment and IFPD groups (P < 0·001). No significant differences were found between groups in educational achievement level (P = 0·81), past usage of RPD (P = 0·66) and symmetry of arch (P = 0·12). All subjects with symmetrical arches (n = 29) reported that they had no preferred chewing side, while 62·9% (73/116) of those with asymmetric arches preferred to chew on the side with more occluding pairs (P < 0·001).

Analysis of SDA subtype (Table 2) indicated that only 3·3% (1/30) of subjects with type I sought prosthetic treatment, which was significantly less than those with type II (58·1%; 36/62) and type III (92·5%; 49/53) (P < 0·001) (Table 5).

Logistic regression analysis of the total subjects identified young age, increased number of missing OU, asymmetric arch and presence of chewing
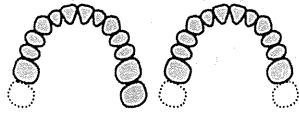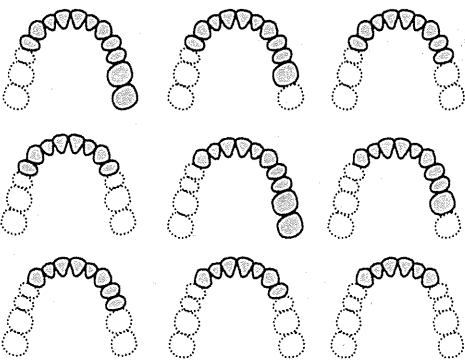
masticatory function (23). At baseline, a questionnaire was given to the subjects to record the duration of SDA without replacement, past usage of RPD, educational level, preferred chewing side and whether they had complaint about their chewing ability. Each subject received a written and oral description of the experimental procedures, and informed consent was obtained prior to enrolment in the study. All experimental procedures were approved by the ethical committee of each university. In this report, characteristic of each group and the factors related to prosthetic restoration decisions are presented. Evaluation of treatment effects on OHRQoL, chewing ability and objective masticatory function will be reported in separate papers.

Statistical analysis

Comparisons between groups of gender distribution, duration of SDA, chewing complaint, educational level, past usage of RPD and symmetry of arch were made using chi-square test or Fisher's exact test. Comparisons of mean age and number of missing OUs between groups were performed using one-way analysis of variance (ANOVA) with Tukey's test. SDA was then classified into three subtypes, based on the pattern of missing posterior teeth (Table 2), to test the effect of SDA type on prosthetic restoration decisions using Fisher's exact test. To determine factors related to prosthetic restoration on SDA, logistic regression analysis was performed using prosthetic restoration/no treatment as the outcome, and gender, age, number of missing OU, symmetry of arch and chewing complaint as predictors. In addition, logistic regression analysis was performed using chewing complaint as the outcome, and gender, age, number of missing OU and symmetry of arch as predictors. The primary hypothesis in this study was that an increase in missing OU was associated with selection of prosthetic

Table 2. Definition for subtypes of shortened dental arches

Subtype	Pattern of missing posterior teeth	Missing occlusal units	Examples of maxillary arch
Type I	2nd molar(s) was/were missing. 1st molars were present on bilateral side of the mouth.	2,4	
Type II	1st and 2nd molars were missing on the unilateral/ bilateral side of the mouth. 1st and 2nd premolars were present on the bilateral side of the mouth.	4,6,8	
Type III	1st and 2nd molars were missing on the unilateral/ bilateral side of the mouth. 1st and/or 2nd premolar(s) was/were missing.	5–12	

addition, randomised controlled trials carried out by other researchers suggest that restoration with cantilever-fixed partial dentures for the SDA is more favourable than treatment with removable partial dentures (RPDs) in terms of patient satisfaction, oral health-related quality of life (OHRQoL), longevity, prevention of caries and periodontal disease affecting the abutment teeth (3–8). Some cross-sectional, case–control and prospective studies suggest that prosthetic treatment with RPDs does not improve oral function and OHRQoL of SDA patients (9–13). A review concluded that patients are more concerned about their appearance rather than chewing. Consequently, the demand for the replacement of missing posterior teeth may not be a priority from the patients' view (14). To date, the SDA concept that a recommended treatment option for SDA is no restoration is widely accepted in European countries as an alternative option for the treatment of partial edentulism from a patient-centred view (15–17).

Although Japanese dentists are well aware of the SDA concept, its clinical application seems to be limited compared to Sweden (18). A number of clinical studies on SDA patients have been carried out in European countries (2–10, 12, 13); however, findings in Japanese SDA patients are limited in terms of quality of life (11). The health insurance system and socio-economic background in Japan differ from those in European countries. Therefore, the application of the SDA concept in Japan is still under debate. In 2003, the Japan Prosthodontic Society held a symposium focusing on indications and limitations of the SDA concept in Japan and concluded that more evidence based on clinical studies is needed to validate application of the SDA concept in Japan (19, 20). Following this symposium, a multicentre cross-sectional study was carried out to investigate the relationship between missing OU and OHRQoL in Japanese SDA patients (21, 22). The results of the study indicated that a greater number of missing OUs were associated with impairment of OHRQoL and that occluding pairs of first molars are considered important to maintain adequate OHRQoL level. Following this study, a research group was formed from seven universities located at major cities in Japan. This project aimed at investigating the effect of prosthodontic treatment with RPDs or implant-supported fixed partial dentures (IFPD) on OHRQoL and masticatory function in SDA patients. Although a number of clinical studies have been carried out to investigate the effect of prosthetic treatment in SDA patients (3–13), the factors

related to prosthetic restoration have not been identified. Thus, the present study investigated the factors related to prosthetic treatment decisions for SDA based on the data obtained from baseline assessment.

Materials and methods

This study employed a multicentre prospective design. SDA patients who met the prescribed inclusion and exclusion criteria as shown in Table 1 were consecutively enrolled in the study from seven university-based dental hospitals (Tokyo Medical and Dental University, Osaka University, Showa University, Kyushu University, Hiroshima University, Tohoku University and Okayama University). All patients participated in this study were recruited from prosthetic clinics. SDA patients who did not seek prosthetic treatment but regular oral maintenance care at prosthetic clinics were also enrolled in the study. The subjects chose no treatment (wait and see) or treatment with RPD or IFPD for their edentulous spaces on entry. OHRQoL, perceived chewing ability and objective masticatory function were assessed at baseline and reassessed during regular check-up for the no-treatment group and after treatment for the treatment group. A masticatory performance test using a gummy jelly as a test food was employed for the assessment of objective

Table 1. Criteria for subject enrolment in the study

Criteria	
Inclusion criteria	Kennedy class I or class II partially edentulous areas posterior to canines with no modification spaces (2–12 missing occlusal units)
	Kennedy class I or class II partially edentulous areas untreated for at least 1 month
	Intact anterior dental arch restorable with fixed partial dentures or implant-supported fixed partial dentures
Exclusion criteria	Acute dental and periodontal diseases
	Current usage of removable partial dentures
	Posterior teeth treated with fixed partial denture pontic or implant-supported fixed partial denture
	Planned to be restored with cantilever-fixed partial denture

Factors related to prosthetic restoration in patients with shortened dental arches: a multicentre study

K. FUEKI*, Y. IGARASHI*, Y. MAEDA[†], K. BABA[‡], K. KOYANO[§], Y. AKAGAWA[¶], K. SASAKI**, T. KUBOKI[††], S. KASUGAI[‡‡] & N. R. GARRETT[§§¶¶] *Section of Removable Partial Denture Prosthodontics, Graduate School of Medical and Dental Sciences, Tokyo Medical and Dental University, Tokyo, [†]Division of Oromaxillofacial Regeneration, Graduate School of Dentistry, Osaka University, Osaka, [‡]Department of Prosthodontics, School of Dentistry, Showa University, Tokyo, [§]Section of Removable Prosthodontics, Division of Oral Rehabilitation, Graduate School of Dentistry, Kyushu University, Kyushu, [¶]Department of Advanced Prosthodontics, Graduate School of Biomedical Sciences, Hiroshima University, Hiroshima, **Division of Advanced Prosthetic Dentistry, Graduate School of Dentistry, Tohoku University, Sendai, [††]Department of Oral Rehabilitation and Regenerative Medicine, Graduate School of Medicine, Dentistry and Pharmaceutical Sciences, Okayama University, Okayama, [‡‡]Section of Oral Implantology and Regenerative Dental Medicine, Graduate School of Medical and Dental Sciences, Tokyo Medical and Dental University, Tokyo, Japan, [§§]The Jane and Jerry Weintraub Center for Reconstructive Biotechnology and the Division of Advanced Prosthodontics, Biomaterials and Hospital Dentistry, UCLA School of Dentistry, Los Angeles, CA and [¶¶]Veterans Administration Greater Los Angeles Healthcare System, Los Angeles, CA, USA

SUMMARY The aim of this study was to identify the factors related to prosthetic restoration in patients with shortened dental arches (SDA). SDA patients with 2–12 missing occlusal units were consecutively enrolled from seven university-based dental hospitals in Japan. Of the 145 subjects (mean age; 63·4 years), 41% chose no treatment and 59% sought to replace their edentulous spaces with removable partial dentures or implant-supported fixed partial dentures. Restoration decisions were related to tooth loss patterns. Only 3% of subjects missing just second molar(s) sought to receive prosthetic treatment, while the percentage increased to 58% in subjects who were missing first and second molars and 93% in subjects missing premolar(s). Logistic regression analyses found that young age, increased number of missing occlusal units, asymmetric arch and presence of chewing complaint were significant predictors for prosthetic restoration ($P < 0.05$). Increased number of missing occlusal units and asymmetric arch were significant predictors for the presence of chewing complaint ($P < 0.05$). These results suggest that perceived impairment of chewing ability owing to missing occlusal units is a critical factor for prosthetic restoration in SDA patients.

KEYWORDS: shortened dental arch, prosthetic treatment, occlusal unit, multicentre study

Accepted for publication 20 October 2010

Introduction

Replacement of missing teeth and maintenance of 28 teeth has been believed as the traditional treatment goal. In the early 1980s, Käyser (1) named partial edentulism in which the most posterior teeth are missing as shortened dental arch (SDA), and he proposed that SDA patients with at least four occlusal units (OUs) have sufficient adaptive capacity to maintain oral function. A pair of occluding premolars corresponds to one unit, and a pair of occluding molars corresponds to two units (1). The Käyser/Nijmegen group carried out cross-sectional studies and longitudinal studies in Netherlands and Tanzania to investigate oral function, signs and symptoms of temporomandibular disorders, occlusal stability and periodontal support in SDA patients (2). The results of these studies supported the SDA concept proposed by Käyser. In

35. Hansson S, Werke M. The implant thread as a retention element in cortical bone: The effect of thread size and thread profile. A finite element study. *J Biomech* 2003; 36:1247-1258.

36. Black J. "Push-out" tests. *J Biomed Mater Res* 1989; 23:1243-1245.

37. Dhert WJ, Verheyen CC, Braak LH, et al. A finite element analysis of the push-out test: Influence of test conditions. *J Biomed Mater Res* 1992;26:119-130.

38. Weinberg LA. Therapeutic biomechanics concepts and clinical procedures to reduce implant loading. Part I. *J Oral Implantol* 2001;27:293-301.

39. Woo I, Le BT. Maxillary sinus floor elevation: Review of anatomy and two techniques. *Implant Dent* 2004;13: 28-32.

Correspondence: Dr. Malik Hudieb, Department of Oral Implantology and Regenerative Dental Medicine, Tokyo Medical and Dental University, 1-5-45 Yushima, Bunkyo, Tokyo 113-8549, Japan. Fax: 81-3-58034664; e-mail: malik.i.h.irm@tmd.ac.jp.

2. Rasmusson L, Kahnberg KE, Tan A. Effects of implant design and surface on bone regeneration and implant stability: An experimental study in the dog mandible. *Clin Implant Dent Relat Res* 2001;3:2-8.

3. Abrahamsson I, Berglundh T. Tissue characteristics at microthreaded implants: An experimental study in dogs. *Clin Implant Dent Relat Res* 2006;8:107-113.

4. Berglundh T, Abrahamsson I, Lindhe J. Bone reactions to longstanding functional load at implants: An experimental study in dogs. *J Clin Periodontol* 2005; 32:925-932.

5. Wennström JL, Ekestubbe A, Gröndahl K, Karlsson S, Lindhe J. Implant-supported single-tooth restorations: A 5-year prospective study. *J Clin Periodontol* 2005; 32:567-574.

6. Lee DW, Choi YS, Park KH, Kim C-S, Moon I-S. Effect of microthread on the maintenance of marginal bone level: A 3-year prospective study. *Clin Oral Implants Res* 2007;18:465-470.

7. Palmer RM, Palmer PJ, Smith BJ. A 5-year prospective study of Astra single tooth implants. *Clin Oral Implants Res* 2000;11:179-182.

8. Schrotenboer J, Tsao YP, Kinariwala V, Wang HL. Effect of microthreads and platform switching on crestal bone stress levels: A finite element analysis. *J Periodontol* 2008;79:2166-2172.

9. Hansson S, Halldin A. Re: effect of microthreads and platform switching on crestal bone stress levels: A finite element analysis (letter to the editor). *J Periodontol* 2009;80:1033-1035; authors' response 1035-1036.

10. Isidor F. Loss of osseointegration caused by occlusal load of oral implants. A clinical and radiographic study in monkeys. *Clin Oral Implants Res* 1996;7: 143-152.

11. Isidor F. Histological evaluation of peri-implant bone at implants subjected to occlusal overload or plaque accumulation. *Clin Oral Implants Res* 1997;8:1-9.

12. Carlsson GE. Critical review of some dogmas in prosthodontics. *J Prosthodont Res* 2009;53:3-10.

13. Hobkirk JA, Wiskott HWA, Working Group 1. Biomechanical aspects of oral implants. Consensus report of Working Group 1. *Clin Oral Implants Res* 2006; 17(Suppl. 2):52-54.

14. Duyck J, Rønold HJ, Van Oosterwyck H, Naert I, Vander Sloten J, Ellingsen JE. The influence of static and dynamic loading on marginal bone reactions around osseointegrated implants: An animal experimental study. *Clin Oral Implants Res* 2001;12:207-218.

15. Miyata T, Kobayashi Y, Araki H, Ohto T, Shin K. The influence of controlled occlusal overload on peri-implant tissue. Part 3: A histologic study in monkeys. *Int J Oral Maxillofac Implants* 2000;15:425-431.

16. Gotfredsen K, Berglundh T, Lindhe J. Bone reactions adjacent to titanium implants subjected to static load. A study in the dog (I). *Clin Oral Implants Res* 2001;12: 1-8.

17. Miyata T, Kobayashi Y, Araki H, Motomura Y, Shin K. The influence of controlled occlusal overload on peri-implant tissue: A histologic study in monkeys. *Int J Oral Maxillofac Implants* 1998;13:677-683.

18. Hudieb MI, Wakabayashi N, Suzuki T, Kasugai S. Morphologic classification and stress analysis of the mandibular bone in the premolar region for implant placement. *Int J Oral Maxillofac Implants* 2010;25: 482-490.

19. Petrie CS, Williams JL. Comparative evaluation of implant designs: Influence of diameter, length, and taper on strains in the alveolar crest. A three-dimensional finite-element analysis. *Clin Oral Implants Res* 2005;16:486-494.

20. Kitamura E, Stegaroiu R, Nomura S, Miyakawa O. Influence of marginal bone resorption on stress around an implant — A three-dimensional finite element analysis. *J Oral Rehabil* 2005;32:279-286.

21. Veltri M, Ferrari M, Balleri P. One-year outcome of narrow diameter blasted implants for rehabilitation of maxillas with knife-edge resorption. *Clin Oral Implants Res* 2008;19:1069-1073.

22. O'Mahony AM, Williams JL, Spencer P. Anisotropic elasticity of cortical and cancellous bone in the posterior mandible increases peri-implant stress and strain under oblique loading. *Clin Oral Implants Res* 2001;12:648-657.

23. Huang HL, Chang CH, Hsu JT, Fallgatter AM, Ko CC. Comparison of implant body designs and threaded designs of dental implants: A 3-dimensional finite element analysis. *Int J Oral Maxillofac Implants* 2007; 22:551-562.

24. Al-Sukhun J, Kelleway J. Biomechanics of the mandible: Part II. Development of a 3-dimensional finite element model to study mandibular functional deformation in subjects treated with dental implants. *Int J Oral Maxillofac Implants* 2007;22:455-466.

25. Mericske-Stern R, Assal P, Mericske E, Bürgin W. Occlusal force and oral tactile sensibility measured in partially edentulous patients with ITI implants. *Int J Oral Maxillofac Implants* 1995;10:345-353.

26. Norton MR. Marginal bone levels at single tooth implants with a conical fixture design. The influence of surface macro- and microstructure. *Clin Oral Implants Res* 1998;9:91-99.

27. Ona M, Wakabayashi N. Influence of alveolar support on stress in periodontal structures. *J Dent Res* 2006; 85:1087-1091.

28. Brunski JB. In vivo bone response to biomechanical loading at the bone/dental-implant interface. *Adv Dent Res* 1999;13:99-119.

29. Hsu ML, Chen FC, Kao HC, Cheng CK. Influence of off-axis loading of an anterior maxillary implant: A 3-dimensional finite element analysis. *Int J Oral Maxillofac Implants* 2007;22:301-309.

30. Kim Y, Oh TJ, Misch CE, Wang HL. Occlusal considerations in implant therapy: Clinical guidelines with biomechanical rationale. *Clin Oral Implants Res* 2005; 16:26-35.

31. Sütpideler M, Eckert SE, Zobitz M, An KN. Finite element analysis of effect of prosthesis height, angle of force application, and implant offset on supporting bone. *Int J Oral Maxillofac Implants* 2004;19:819-825.

32. Guo EX. Mechanical properties of cortical bone and cancellous bone tissue. In: Cowin SC, ed. *Bone Mechanics Handbook*. Boca Raton, FL: CRS press; 2001:10/1-23.

33. Frost HM. From Wolff's law to the mechanostat: A new "face" of physiology. *J Orthop Sci* 1998;3:282-286.

34. Lekholm U, Sennerby L, Roos J, Becker W. Soft tissue and marginal bone conditions at osseointegrated implants that have exposed threads: A 5-year retrospective study. *Int J Oral Maxillofac Implants* 1996;11: 599-604.
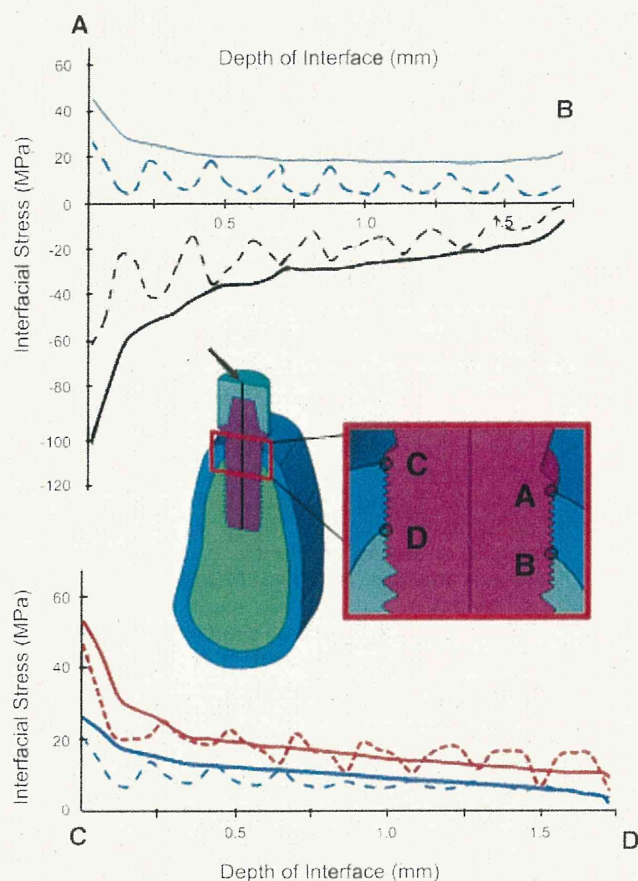
Figure 5.

Interfacial stresses on the compression (upper graphs) and tension (lower graphs) sides under the 30° oblique load. The bone–implant interfacial compressive (black), shear (blue), and tensile (red) stresses in the cortical bone along the lingual wall for compressive side of the microthreaded model (dashed lines) and smooth model (solid lines) under the 30° oblique load. The shear and tensile stresses were represented as positive values, whereas the compressive stress was shown as negative values.

implant (i.e., failure of the interface because of shear stress) may not be applicable. This is actually because of the simplicity of methods used in this issue. For example, most push-out tests did not really measure the shear strength of the bone–implant interface; instead, they reported a value that although called "pushout strength," is a combination of various fixation principles (friction, mechanical interlock, and chemical bonding).[36,37] Accordingly, the debonding was not allowed in this study under shear stress.

In addition, cyclic fatigue loading should be considered if a structural model was made to account for changes in the bone–implant interface with degradation or failure of osseointegration. An earlier animal study described a greater bone response revealed when rabbit tibiae was loaded dynamically than statically.[14]

Further biologic studies regarding the effects of the tensile and shear stresses on the interfacial failure are encouraged to establish a comprehensive understanding of the role of occlusal loads in preserving peri-implant tissues.

The findings of this study demonstrated the effectiveness of the microthread design not only in withstanding off-axis loading but also supporting the hypothesis of the effect of threads in transforming shear stress into a compressive stress. Reducing shear stress under off-axis loading indicates the benefit of microthread design especially when a larger horizontal force component is expected, such as in the anterior maxillary region[38] or when implants are tilted because of the presence of anatomic limitations.[39]

CONCLUSIONS

Off-axis occlusal loads create compression and tension fields in the crestal bone, and are typically located on the opposite sides across the implant. In the smooth-surface implant, the direction of the principal stresses at the bone–implant interface was found to be oblique to the interface and affected by the loading angle, whereas those were consistently perpendicular to the lower flank of microthreads under different loading angles in the microthread implant, suggesting that the stress at the microthread interface was insensitive to the loading angle and indicating larger shear stress at the bone–implant interface around the smooth implant. Also, the microthread design was found to be more effective in reducing shear stress under off-axis loading, which dominates in the oral cavity. However, higher peak compressive stress and strain around the microthread implant were found to be localized in a smaller bone volume compared to the smooth implant. These results collectively might demonstrate the biomechanical rationale of microthread design over smooth surfaces in reducing the risks of marginal bone loss caused by overloading.

ACKNOWLEDGMENTS

REFERENCES

1. Hansson S. The implant neck: Smooth or provided with retention elements. A biomechanical approach. *Clin Oral Implants Res* 1999;10:394-405.
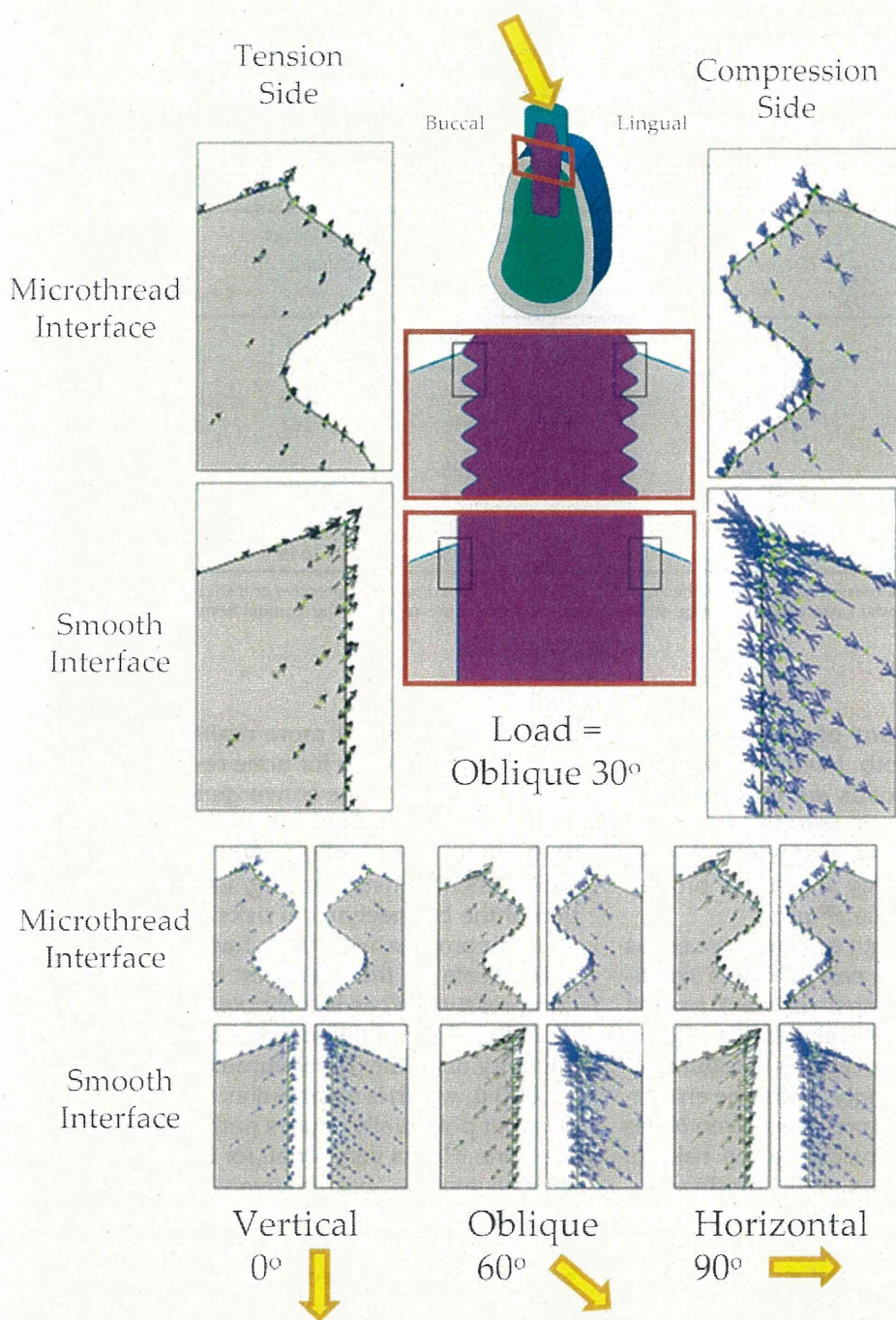
Figure 4.

Stress arrow graphics at the cervical level of the cortical bone on the tension and compression sides. The direction and magnitude of the principal stress at each element in the crestal bone of the buccal (tension) and lingual (compression) sides are shown in the bucco-lingual section at the mesio-distal center of each implant under vertical (0°), 30° oblique, 60° oblique, and horizontal (90°) loadings. Black arrows represent the first principal (tensile) stress; blue arrows indicate the third principal (compressive) stress. Length of each arrow represents relative magnitude of stress that is projected on the two-dimensional plane. Figures with black and red squares in the middle indicate the site of the arrow graphics.

this study consists of that shown in a previous FE study.[35] It is now clear that the location of the first thread relative to the bone surface affects the stress distribution in the cervical region; however, the effect was limited to this region and did not seem to have a negative effect because the volume of bone that exhibited high strain (red area in Fig. 2) was smaller in the microthread model than in the smooth model (Table 1).

However, in this study, the modeling of the bone–implant interface was performed on the assumption of a perfect bonding because no detachment was allowed under tensile or shear stresses. This has been assumed because of the absence of reliable interfacial tensile and shear strength data. Regarding the bone–implant interfacial tensile strength, previous studies reported a range of 1 to 4 MPa;[28] however, in most of these studies, a flat implant model was used and the variability in bone–implant contact percentage was not considered. Bone–implant contact percentage greatly varies among different surfaces and designs. However, the debonding at the tension side has never been reported clinically under functional occlusal forces. Moreover, because the microthreaded implants have shown larger bone–implant contact percentage,[3] it is expected that microthreaded implants will have larger interfacial tensile strength.

Furthermore, comparing the results of this study with the available bone–implant interfacial shear strength to predict whether there will be debonding or sliding of the

Table 1.

Maximum Stress and Strain Values in the Compressive and Tensile Halves of the Crestal Bone Surrounding the Microthread and Smooth Implant Under Vertical, 30°, 60° Oblique, and Horizontal Loading

Model	Force Direction (degree)	Compressive Side					Tensile Side	
		Compressive Stress (MPa)	Tensile Stress (MPa)	Shear Stress (MPa)	Compressive Strain (μ strain)	Large Strain Volume (mm³)	Tensile Stress (MPa)	Shear Stress (MPa)
Microthread	0	42.49	87.77	28.95	4,740	1.38E-04	77.41	1.6
	30	201.9*	142.1	44.6*	10,990*	0.033431	70.1	21.8
	60	259.6	116.5	63.7	14,515	0.215624	183.3	52.2
	90	248.0	137.3	65.7	14,176	0.219261	248.1	68.94
Smooth	0	87.6	59.6	21.3	3,898	0	59.1	2.7
	30	140.8	81.7	49	8,214	0.041591	58.7	25.3
	60	201.6	95.4	83.5	14,041	0.244157	145.1	59.2
	90	206.3	80.4	85.7	14,373	0.242616	199.8	78.2

The maximum values were indicated at the mesio-distal center of the implants, except for the maximum compressive and shear stresses and the maximum compressive strain in the microthread model (asterisks). The large strain volume represents the region of the cortical bone that showed the maximum compressive strain >4,000 μ.

analysis, considerable amount of shear stress is transmitted across the smooth interface, whereas for the microthread implant loads are transferred to compressive stresses (at the compression side) perpendicular to the lower flank of each microthread. These results were confirmed by the stress profiles along the bone–implant interface (Fig. 5).

Transferring occlusal loads into compressive stress around the microthread implant can provide a significant benefit because bone is most resistant against the compressive forces.[32] Interfacial failure and bone resorption under different stress types is attributed to different mechanisms. Accordingly, it may be erroneous to emphasize the peak compressive or von Mises equivalent stresses without considering the risks of the tensile and the shear stresses at the interface.

The results of this analysis revealed that incorporating microthreads in the implant neck resulted in higher peak compressive stress and strain values in the peri-implant bone structures under off-axis loading. These findings are consistent with those of a previous two-dimensional FE study in which maximum von Mises stress was higher in the crestal bone around microthread implant.[8] However, the high stress and strain magnitude were found to be limited to a small region localized at the crestal bone around the implant neck. Although the estimation of the maximum equivalent (von Mises) and the principal stresses has been frequently used to assess failure risks of biomaterials and the peri-implant bone tissues, evaluating the bone volume that exhibited high stress or strain and the stress distribution pattern along the

interface may reflect more realistic quantitative and qualitative measures for bone resorption risks. Moreover, the results of the convergence tests suggest that the peak stress that is usually used in previous comparisons was highly dependent of the mesh size, and thus does not ensure validity for quantitative evaluation of the biomechanical risks.

The compressive strain has often been used as a risk scale on the basis that bone resorption under compressive forces is attributed to the accumulation of induced microdamage that exceeds the bone's capacity of repair. The volume of the high strain level >4,000 μ, which is regarded as a mechanical stimulation that potentially causes pathologic overloading to the bone,[33] was very small for both microthread and smooth models, but relatively larger in the case of the smooth-neck model. This may cancel the proposed advantage of the lower stress and strain values around the smooth-neck implant, which was reported in the previous study[8] and confirmed in this research.

Incomplete coverage of implant microthreads or macrothreads may result because of the narrow dimension of the crestal region and the curved nature of the alveolar bone. This is considered to be an acceptable situation as reported in previous clinical studies with different follow-up periods.[21,34] The three-dimensional modeling of the implant and the bone in this study allowed for simulating this situation, which was not shown in the previous two-dimensional models. In the microthreaded implant, the peak compressive stress was shifted from the mid line to the exposed thread region. The location of peak stress in

Low ▬▬▬▬▬▬▬ High
Compressive Strain
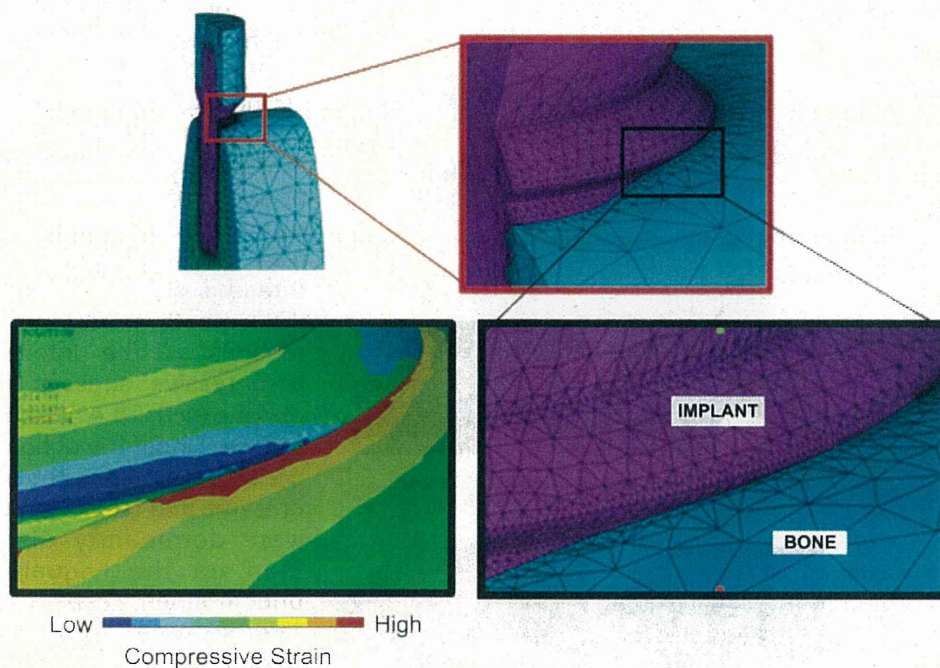
Figure 3.

The maximum compressive strain distributions of the microthread and the crestal bone in the disto-lingual surrounding of the microthread implant. The maximum compressive strain of the bone appeared in the region just under the first microthread that was exposed from the crestal edge.

stress in the lower flank of the microthreads, which was higher than that in the smooth model at the same vertical level.

The peak compressive strains of the bone along the interface on the lingual and buccal sides are shown in Table 1.

DISCUSSION

Altering the surface structure of dental implants is an effective way to preserve the peri-implant marginal bone.[26] Microthread design is considered as a retentive element and macro-roughness[1] has demonstrated the beneficial effect of reducing marginal bone resorption in clinical and animal studies.[3,6]

The effect of loading angle on the magnitude and directions of the interfacial stress around the microthread implant was not clear. Although the implant fixtures are usually installed perpendicularly to the occlusal plane, implants are susceptible also to oblique and horizontal loading. These loads on the implant create two typically shown stress fields in the crestal bone: the compression and tension fields, which are located on the opposite sides across the implant and characterized by domination of the principal compressive and tensile stresses, respectively. Such stress fields are also created in the periodontal structures of a natural tooth,[27] but are different from

those of the implant vicinity, in that the periodontal ligament acts as a cushion and absorbs tensile and compressive stresses. In contrast, the bone–implant interface is so rigid that the stress increases on the off-axis loading and potentially causes interfacial failures.[28] To comprehensively evaluate the biomechanical aspects of microthread design, the magnitude and direction of different interfacial stresses along with high-strain bone volumes under different loading angles were analyzed in this study.
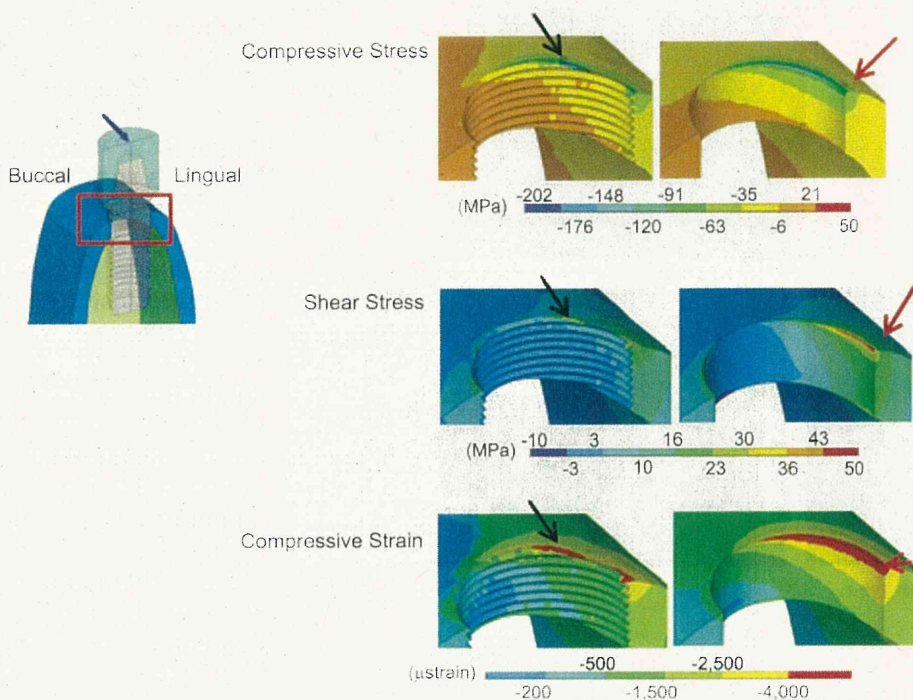
On vertical loading, the microthread implant showed lower compressive but higher shear and tensile stress values compared to the smooth implant. These results disagree with a previous FE study[1] in which vertical forces only were applied and resulted in lower peak shear stress in the microthread model. This disagreement is probably because of the differences in the morphology of the alveolar bone and material properties assigned. However, a marked increase in the first and third principal and shear stress values in both models was observed as the loading angle increased in the oblique and horizontal loading cases. Off-axis loading was found to be more destructive to the bone–implant interface.[29-31] Interestingly, under off-axis loading, the microthread implant in this study generated lower maximum shear but higher compressive stress values.
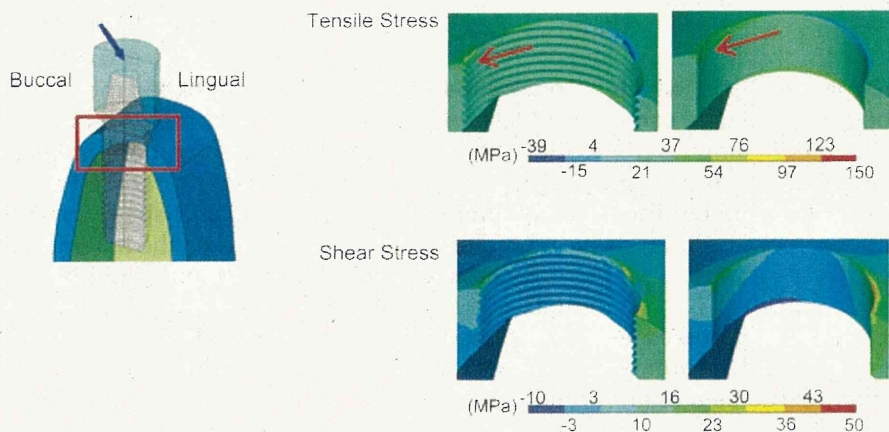
Also, the direction of the principal stresses at the microthread interface was consistently perpendicular to the lower thread flank regardless of the loading direction. In contrast, the direction of the principal stresses in the smooth model was oblique to the interface and affected by the loading angle. As the loading angle increased (i.e., larger horizontal component), interfacial stresses tended to be more oblique to the interface.

Oblique interfacial stress direction represents a resultant force that can be analyzed into the two basic force components: the first is perpendicular to the interface and represents the compressive or tensile stress, and the second is parallel with the interface and represents the shear stress. According to this

A Compression Side

Compressive Stress

(MPa) -202   -148   -91   -35   21
        -176   -120   -63   -6   50

Shear Stress

(MPa) -10   3   16   30   43
        -3   10   23   36   50

Compressive Strain

(µstrain)   -500   -2,500
        -200   -1,500   -4,000

B Tension Side

Tensile Stress

(MPa) -39   4   37   76   123
        -15   21   54   97   150

Shear Stress

(MPa) -10   3   16   30   43
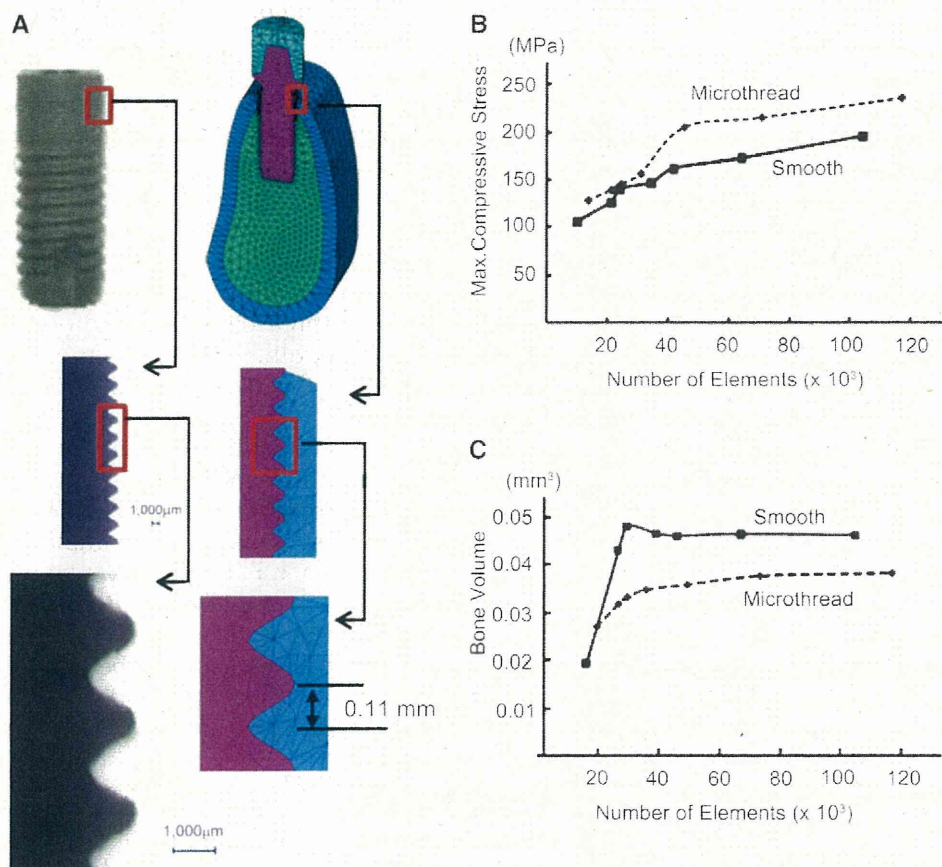   -3   10   23   36   50

Figure 2.
A and B) The compressive, tensile, and shear stress distributions and the compressive strain distributions in the cervical cortical bone under the 30° oblique load with microthread and smooth models. The distal half of each symmetric section is viewed from the mesial side, with the focus on the interfacial bone surface. Figures on the left indicate the viewing angle and the region (red square) in the contour graphics on the right. Blue arrows indicate the direction of occlusal forces. Each contour graphic was divided into nine parts, with different colors according to the stress or strain levels, shown in a scale below each figure. Red arrows indicate the location of the maximum stress that appeared at the mesio-distal center of each implant. Black arrows indicate the location of the maximum stress that deviated from the mesio-distal center of each implant.

sides of the interface, with the highest stress located at the top of the ridge. In the microthread model, large compressive stresses were shown mostly under the lower flank of each microthread and the directions of the stresses were perpendicular to the thread surface, whereas in the smooth model the directions of the interfacial compressive stresses were oblique (with 58.4°) to the interface. Under the oblique or horizontal loadings, the compressive and tensile stresses were dominantly distributed on the lingual and buccal sides, respectively. The stresses were again perpendicular to the lower surface of each microthread, whereas in the smooth model the stress directions were oblique to the interface with 50.5°, 45.1°, and 46.8° under the 30°, 60°, and horizontal loading, respectively.

The peak compressive and shear stresses on the interface along the lingual wall and the peak tensile and shear stresses along the buccal wall, both at the mesio-distal center under the 30° oblique load, are graphed in Figure 5. All stresses peak at the top of the crestal bone. The microthread model exhibited decreases of the stresses with a wavy pattern as downward along the interface, whereas the stresses in the smooth model decreased with a gradual curve. In the wavy curve of the microthread model, the bottom of each wave corresponded to the thread root, whereas the prominence of each wave corresponded to the point where the lower flank passes to the curved thread crest. The microthread model indicated lower peak stresses than the smooth model along the whole interface, except for the tensile

The principal stresses at each node in the cortical bone were shown in the form of stress arrows on the bucco-lingual section at the mesio-distal center of each implant (Fig. 4). Under the vertical loading, the compressive stress was evenly distributed on both

Figure 1.
The meshed FE model of the implant and the bone (A) and the convergence tests (B and C). Cancellous bone (green mesh) surrounded by a layer of cortical bone (blue mesh). Light microscopic images of the microthread morphology in the implant fixture were traced to create the neck part of the three-dimensional FE model of the implant (A). The convergence test of the microthread and smooth implant neck models of this study. The maximum third principal stress at the crestal bone (B) and bone volumes that exhibited the maximum compressive strain >4,000 μ (C) were used as the variable measures. Seven iterations by mesh refinement were calculated up to 120,000 elements for each model.

minimum principal stress), tensile (first or maximum principal stress), and shear stress and strain generated in the bone were analyzed.

RESULTS

For the convergence tests, seven iterations by mesh refinement were calculated for each model. The peak compressive stress values and the bone volume that exhibited a high compressive strain >4,000 μ as a function of the number of elements are shown in Figures 1B and 1C. As the number of elements increased, both models revealed an increase in the peak compressive stress without showing a plateau even with using ≈120,000 elements. The curves of the high strain bone volumes revealed a well-developed plateau after the number of elements was >≈40,000. This indicates that the volume of high strain is insensitive to further refinement of the mesh. Based on these results, the element edge size was set equal to 0.03 mm for the interface. Accordingly, the final microthread model was composed of 70,060 elements and 13,867 nodes, and the smooth model was of 63,568 elements and 13,744 nodes.

directions at the nodes on the distal bone surface. The implants were rigidly anchored in the bone models along the entire interface, and the same type of contact was provided at the prosthesis–abutment interface. A static load in one of the four directions (vertical [0°], 30°, and 60° oblique from buccal to lingual, and horizontal [90°] angles to the long axis of each implant) was applied to the center of the occlusal surface of the superstructure. However, the 30° oblique load, which corresponded with the direction of occlusal forces in the premolar region was used for general discussion. Because the point of load application is included in the symmetry boundary conditions, each input load was doubled during computations. The resultant load (200 N) was used to simulate the average maximum occlusal load for fixed partial prosthesis supported by implants in the premolar region.[25] The directions and magnitudes of the maximum compressive (third or

The compressive, shear, and tensile stress distributions in the bone under the 30° oblique load are shown in Figure 2. The location of the maximum stress in the smooth model was at the top of the crestal cortical bone attached to the mesio-distal center of the implant, whereas those of the peak compressive and shear stresses in the microthread model were deviated distally from the mesio-distal center (black arrows in the Fig. 2).

Figure 3 shows the peak compressive stress appeared in the region right under the flank of the first microthread, which was exposed from the crestal edge in the disto-lingual region. The maximum stress values in the microthread and smooth models on the lingual and buccal crestal bone under all loading angles are shown in Table 1.

as one of the important causes of implant failures.[10,11] However, a causative relationship between implant failure and occlusal forces has not been convincingly demonstrated.[12,13] Animal studies provided conflicting results in this issue. Under extensive occlusal and cyclic loading, marginal bone resorption has been demonstrated in the absence of peri-implant tissue inflammation.[10,14,15] However, experimental studies using different animal models have shown that occlusal stress does not cause significant peri-implant bone loss in the absence of peri-implant infection.[16,17]

Although various attempts have been made to assess the effect of occlusal loads on peri-implant bone loss, the "overloading" has not been well defined in terms of mechanical stress at the bone–implant interface. Because the progress of the marginal bone loss occurs as a result of the bone resorption or loss of the bone–implant contact at the interface (interfacial failure), the magnitude and direction of the stress should be fully investigated to assess potential association between the overloading and the marginal bone loss.

The objective of this study is to assess the effects of microthread design and loading angle on the direction and magnitude of the interfacial, principal (stresses in the principal planes), and shear stresses at the bone–implant interface around the implant. The results were analyzed to understand stress-transferring mechanisms from different implant surfaces to the supporting bone, and to test a hypothesis that the microthread structure reduces the risk of interfacial failures.

MATERIALS AND METHODS

Construction of Three-Dimensional Models

Three-dimensional FE models representing two implants, one with microthreads in the neck region and the other with a smooth neck, were constructed. A microthreaded implant§ with 4-mm diameter and 11-mm length was scanned under a microscope‖ and imported into image analysis software.¶ The outline of the implant was plotted and converted into x and y coordinates, which were imported into the FE software# as keypoints (Fig. 1). For the smooth-neck implant, which served as control, the outline was created by connecting the tops of the microthreads of the microthread model. The two-dimensional images were then extruded around their central axis to produce axisymmetric three-dimensional FE models. The implants were connected to abutment** and simplified cylindrical crown of 7.5-mm height and 5.5-mm diameter, which were created using the same procedure as for the implant.

A three-dimensional FE model of a mandibular bone segment was created based on the most common morphologic model among the nine classifica-

tion groups for the mandibular premolar region in our previous study.[18]

Average dimensions of the cross-sectional outlines at the premolar region based on computed tomography images of 36 patients of that morphology group were used to create x and y plots that described the outline of the external cortical bone surface. The area made from the outline was divided into a cancellous core surrounded by a uniform 1.5-mm thick cortical bone. Each image on the x–y plane was extruded to the z axis to create a three-dimensional model with 15-mm mesio-distal length. Because of the mesio-distal symmetry, only the distal half of the model was constructed.[19,20]

The vertical dimension and the maximum bucco-lingual width of the mandible model at the first premolar region where the implant is being installed were 28.6 and 13.9 mm, respectively. Each implant was vertically embedded on top of the alveolar ridge. The central axis of each implant positioned at the bucco-lingual center. The vertical position was determined so that the microthread was embedded at the highest level of the alveolar crest in the distal cervical bone; this resulted in exposure of a thread at the buccal and lingual ridges.[21]

Material Properties, Meshing, Boundary, and Loading Conditions

The material properties of cortical and cancellous bone were modeled as being transversely isotropic and linearly elastic,[22,23] which describes an anisotropic material. The materials of the implant and prosthetic crown were assumed to be isotropic and linearly elastic with Young moduli and Poisson ratio of 107 GPa and 0.3 for the implant and of 96 GPa and 0.35 for the prosthetic crown, respectively.

A 20-node tetrahedral element was used for the mesh. To determine the valid element numbers and mesh sizes, the convergence test for consistency of solutions was conducted for each model.[24] Two variables were tested: the maximum third principal stress and the volume of cortical bone that exhibited compressive strain >4,000 μ. The mesh was refined several times by reducing the edge size for elements to increase the numbers of nodes at the bone–implant interface where the maximum stress and strain appeared. The least number of elements, over which the variable measures became plateau, was used in this study.

The symmetric boundary conditions were prescribed at the nodes on the mesial plane of the distal half of each model. The models were constrained in all

Magnitude and Direction of Mechanical Stress at the Osseointegrated Interface of the Microthread Implant

Malik I. Hudieb,*† Noriyuki Wakabayashi,† and Shohei Kasugai*†

Background: The mechanism by which the microthread implant preserves peri-implant crestal bone is not known. The objective of this research is to assess the effect of microthreads on the magnitude and direction of the stress at the bone–implant interface using finite element analysis modeling.

Methods: Three-dimensional finite element models representing the microthreaded implant (microthread model) and smooth surface implant (smooth model) installed in the mandibular premolar region were created based on microscopic and computed tomography images. The mesh size was determined based on convergence tests. Average maximum bite force of adults was used with four loading angles on the occlusal surface of the prosthesis.

Results: Regardless of the loading angle, principal stresses at the bone–implant interface of the microthread model were always perpendicular to the lower flank of each microthread. In the smooth model, stresses were affected by the loading angle and directed obliquely to the smooth interface, resulting in higher shear stress. The interfacial stresses decreased gradually in the apical direction in both models but with wavy pattern in the microthread model and smooth curve for the smooth model. Although peak principal stress values were higher around the microthread implant, peri-implant bone volume exhibiting a high strain level >4,000 μ was smaller around the microthread implant compared to the smooth implant.

Conclusion: Stress-transferring mechanism at the bone–implant interface characterized by the direction and profile of interfacial stresses, which leads to more compressive and less shear stress, may clarify the biomechanical aspect of microthread dental implants. *J Periodontol 2011;82:1061-1070.*

KEY WORDS

Bone and bones; dental implant; finite element analysis; occlusal force; stress, mechanical.

* Department of Oral Implantology and Regenerative Dental Medicine, Graduate School, Tokyo Medical and Dental University, Tokyo, Japan.
† Global Center of Excellence Program "International Research Center for Molecular Science in Tooth and Bone Diseases," Tokyo Medical and Dental University.
‡ Department of Removable Prosthodontics, Division of Oral Health Sciences, Graduate School, Tokyo Medical and Dental University.

Microthread structure has been proposed as a bone-retention element at the implant neck to stabilize the peri-implant marginal bone level.[1] Animal experiments have demonstrated larger mineralized bone that comes in contact with implant surface and well-maintained marginal bone levels around microthread implants.[2-4] In clinical studies, radiographic evaluation revealed insignificant amounts of crestal bone loss around microthread implants up to 5 years follow-up.[5-7]

The benefit of microthreads, however, has not been well understood from the mechanical viewpoint. Controversy began with a two-dimensional finite element (FE) study[8] that indicated that the microthread implant had 29% greater maximum von Mises stress at the crestal bone adjacent to the implant than a smooth-neck implant. Opposition was posted to make clarification on some questions regarding the condition at the bone–implant interface, reliability of the material properties, and precision of the modeling.[9] What makes these communications an insoluble issue may partially result from the current lack of knowledge about how mechanical stimulations in terms of stress and strain affect bone retention around implants.

In addition, the contribution of occlusal loads in the pathogenesis of peri-implant marginal bone loss has not been sufficiently verified. Occlusal conditions and overloading have often been proposed

5 Conclusion

In conclusion, our study demonstrated that the thin film sputtered HA coating provides a more favorable surface for bone marrow stromal cell attachment, proliferation and osteoblastic differentiation and function than the surface-modified titanium. The sputtered HA coating also supported osteoclast formation and function which indicated its favorable biodegradability. Therefore, the sputtered HA coating may have an outstanding potential to be used as a drug delivery system in orthopedic and dental applications for more rapid and complete bone-implant integration.

References

1. Lacefield WR. Hydroxyapatite coatings. Ann N Y Acad Sci. 1988;523:72–80.
2. Bidar R, Kouyoumdjian P, Munini E, Asencio G. Long-term results of the ABG-1 hydroxyapatite coated total hip arthroplasty: analysis of 111 cases with a minimum follow-up of 10 years. Rev Chir Orthop Traumatol. 2009;95(8):579–87.
3. Thomas KA. Hydroxyapatite coatings. Orthopedics. 1994;17(3):267–78.
4. Narayanan R, Seshadri SK, Kwon TY, Kim KH. Calcium phosphate-based coatings on titanium and its alloys. J Biomed Mater Res B. 2008;85(1):279–99.
5. Ong JL, Chan DC. Hydroxyapatite and their use as coatings in dental implants: a review. Crit Rev Biomed Eng. 2000;28(5–6):667–707.
6. Zhu X, Son DW, Ong JL, Kim K. Characterization of hydrothermally treated anodic oxides containing Ca and P on titanium. J Mater Sci Mater Med. 2003;14(7):629–34.
7. van Dijk K, Schaeken HG, Wolke JG, Jansen JA. Influence of annealing temperature on RF magnetron sputtered calcium phosphate coatings. Biomaterials. 1996;17(4):405–10.
8. Massaro C, Baker MA, Cosentino F, Ramires PA, Klose S, Milella E. Surface and biological evaluation of hydroxyapatite-based coatings on titanium deposited by different techniques. J Biomed Mater Res. 2001;58(6):651–7.
9. Yang Y, Kim KH, Ong JL. A review on calcium phosphate coatings produced using a sputtering process—an alternative to plasma spraying. Biomaterials. 2005;26(3):327–37.
10. Ozeki K, Mishima A, Yuhta T, Fukui Y, Aoki H. Bone bonding strength of sputtered hydroxyapatite films subjected to a low temperature hydrothermal treatment. Biomed Mater Eng. 2003;13(4):451–63.
11. Ozeki K, Aoki H, Fukui Y. Dissolution behavior and in vitro evaluation of sputtered hydroxyapatite films subject to a low temperature hydrothermal treatment. J Biomed Mater Res A. 2006;76(3):605–13.
12. Minkin C, Marinho VC. Role of the osteoclast at the bone-implant interface. Adv Dent Res. 1999;13:49–56.
13. Gomi K, Lowenberg B, Shapiro G, Davies JE. Resorption of sintered synthetic hydroxyapatite by osteoclasts in vitro. Biomaterials. 1993;14(2):91–6.
14. Doi Y, Shibutani T, Moriwaki Y, Kajimoto T, Iwayama Y. Sintered carbonate apatites as bioresorbable bone substitutes. J Biomed Mater Res. 1998;39(4):603–10.
15. Maniatopoulos C, Sodek J, Melcher AH. Bone formation in vitro by stromal cells obtained from bone marrow of young adult rats. Cell Tissue Res. 1988;254(2):317–30.
16. van't Hof RJ. Osteoclast formation in the mouse coculture assay. In: Helfrich MH, Ralston SH, editors. Bone research protocols. Totowa: Humana Press; 2003. p. 145–52.
17. Ozawa S, Kasugai S. Evaluation of implant materials (hydroxyapatite, glass-ceramics, titanium) in rat bone marrow stromal cell culture. Biomaterials. 1996;17(1):23–9.
18. Saltel F, Destaing O, Bard F, Eichert D, Jurdic P. Apatite-mediated actin dynamics in resorbing osteoclasts. Mol Biol Cell. 2004;15(12):5231–41.
19. Kirstein B. Secretion of tartrate resistant acid phosphatase by osteoclasts correlates with resorptive behavior. J Cell Biochem. 2006;98(5):1085–94.
20. Roodman GD. Advances in bone biology: the osteoclast. Endocr Rev. 1996;17(4):308–32.
21. Sasaki T, Hong MH, Udagawa N, Moriyama Y. Expression of vacuolar H(+)-ATPase in osteoclasts and its role in resorption. Cell Tissue Res. 1994;278(2):265–71.
22. Saftig P, Hunziker E, Wehmeyer O, Jones S, Boyde A, Rommerskirch W, et al. Impaired osteoclastic bone resorption leads to osteopetrosis in cathepsin-K-deficient mice. Proc Natl Acad Sci USA. 1998;95(23):13453–8.
23. Tezuka K, Nemoto K, Tezuka Y, Sato T, Ikeda Y, Kobori M, et al. Identification of matrix metalloproteinase 9 in rabbit osteoclasts. J Biol Chem. 1994;269(21):15006–9.
24. Gori F, Hofbauer LC, Dunstan CR, Spelsberg TC, Khosla S, Riggs BL. The expression of osteoprotegerin and RANK ligand and the support of osteoclast formation by stromal-osteoblast lineage cells is developmentally regulated. Endocrinology. 2000;141(12):4768–76.
25. Lossdörfer S, Schwartz Z, Wang L, Lohmann CH, Turner JD, Wieland M, et al. Microrough implant surface topographies increase osteogenesis by reducing osteoclast formation and activity. J Biomed Mater Res A. 2004;70(3):361–9.
26. Aoki H. Medical applications of hydroxyapatite. Tokyo, St. Louis: Ishiyaku EuroAmerica Inc.; 1994.
27. Ozeki K, Aoki H, Fukui Y. Effect of pH on crystallization of sputtered hydroxyapatite film under hydrothermal conditions at low temperature. J Mater Sci. 2005;40(11):2837–42.
28. Matsumoto T, Okazaki M, Inoue M, Yamaguchi S, Kusunose T, Toyonaga T, et al. Hydroxyapatite particles as a controlled release carrier of protein. Biomaterials. 2004;25(17):3807–12.
29. Nakamura I, Duong IT, Rodan SB, Rodan GA. Involvement of alpha(v)beta3 integrins in osteoclast function. J Bone Miner Metab. 2007;25(6):337–44.
30. Keselowsky BG, Collard DM, García AJ. Integrin binding specificity regulates biomaterial surface chemistry effects on cell differentiation. Proc Natl Acad Sci USA. 2005;102(17):5953–7.
31. Schneider GB, Zaharias R, Stanford C. Osteoblast integrin adhesion and signaling regulate mineralization. J Dent Res. 2001;80(6):1540–4.
32. Zhao C, Irie N, Takada Y, Shimoda K, Miyamoto T, Nishiwaki T, et al. Bidirectional ephrinB2-EphB4 signaling controls bone homeostasis. Cell Metab. 2006;4(2):111–21.
33. Karsdal MA, Neutzsky-Wulff AV, Dziegiel MH, Christiansen C, Henriksen K. Osteoclasts secrete non-bone derived signals that induce bone formation. Biochem Biophys Res Commun. 2008;366(2):483–8.